Carbon Capture Science & Technology 13 (2024) 100280

Contents lists available at ScienceDirect

Carbon Capture Science & Technology

journal homepage: www.elsevier.com/locate/ccst

Full Length Article

Optimization of liquefaction cycles applied to CO_2 coming from onshore pipeline to offshore ship transportation

Alexis Costa [a], Lionel Dubois [b], Diane Thomas [b], Guy De Weireld [a,*]

[a] Thermodynamics and Mathematical Physics Unit, Université de Mons (UMONS), Place du parc 20, 7000 Mons, Belgium
[b] Chemical and Biochemical Process Engineering Unit, Université de Mons (UMONS), Place du parc 20, 7000 Mons, Belgium

ARTICLE INFO

Keywords:
CO_2 transport
CCUS
Optimization
Economic
Exergetic
Liquefaction

ABSTRACT

In the field of the CO_2 transportation for the Carbon Capture, Utilization and Storage (CCUS) process chain, several analyses show that, for a large-scale CO_2 transportation, pipeline transportation is the preferred method on land due to its lower cost. Barges also present a feasible alternative if the capture site is near a waterway. Maritime transport becomes more advantageous than pipelines, particularly over long distances and across ocean. Despite the need to liquefy CO_2 and to add temporary storage facilities for loading and unloading onto ships, beyond a certain distance at fixed CO_2 transported and plant life, ship transport optimal at pressures of 7 or 15 bar depending on the type of vessel. Impurities in CO_2, arising from various industrial processes and variable performances of capture technologies, increase energy consumption during compression and could cause corrosion risks. Specifications for CO_2 ship transport limit the concentration of certain impurities with strict thresholds. Methods for purifying CO_2, such as the two-flash system and stripping column, have been proposed to meet these specifications. The studied CO_2 liquefaction methods show that hybrid cycles, combining open cycle with Joule-Thompson expansion and closed cycle with cooling machine offer reduced energy consumption and improved CO_2 recovery compared to open or closed cycles. In the presence of the maximum threshold of impurities in the pipeline, energy consumption can nearly double from 21.8 kWh/t_{CO2} to 40.9 kWh/t_{CO2}, with the highest recovery rising 98.1 %. This research underscores the importance of optimizing CO_2 transport strategies to facilitate the deployment of CCUS technologies.

1. Introduction

Carbon Capture, Utilization, and Storage (CCUS) has emerged as one of keyways at short and midterm to reduce greenhouse gas emissions and to limit global warming. The process involves capturing carbon dioxide (CO_2) emissions from various industrial sources, preventing their release into the atmosphere (IPCC 2023; IEA 2019).

As an essential part of the CCUS process, transportation phase plays a key role in moving captured CO_2 from a capture site to a storage or utilization site. CO_2 can be transported in various physical states (gas, liquid or supercritical) depending on the means of transportation, with a distinction made between onshore and offshore transport. Onshore transport can be achieved through pipeline, train, truck, or barge, while offshore transport is limited to pipeline or ship (Moe et al., 2020).

When pipelines are used for transport, it is possible to ensure continuous transport, although booster stations may be required for long distances to maintain the minimum transport pressure. CO_2 can be transported in different phases depending on the pipeline network (Wang et al., 2019). Supercritical CO_2 phase is preferred when it is possible, as for new dedicated CO_2 pipeline, due to its properties, which include a high density close to that of liquid and a viscosity comparable to that of gas. Other transport modes (ship, train, truck) are discontinuous and require CO_2 intermediate storage in liquid form; the storage volume being equal to 1 to 2 times the transportable volume (Zhang et al., 2018). The density of liquid CO_2 is predominantly influenced by temperature, rising as temperature decreases. Consequently, weak transport pressure necessitates low temperature, resulting in higher CO_2 density. The triple point of the CO_2, occurring at −56.6 °C, marks the lower temperature limit where solid CO_2 is formed.

When transporting CO_2 over land, pipeline transport is preferred due to its lower cost (Nilsson et al., 2011; Svensson et al., 2004). Other studies indicate that train or truck transport is only economical for small quantities of CO_2 to be transported (Kegl et al., 2021; Psarras et al., 2020), suitable for CO_2 capture unit on small emissions or DAC systems. Barges can be used if the capture site is close to a waterway.

Several studies (Durusut and Joss, 2018; de Kler et al., 2015) have indicated a breakeven point in cost between ship and pipeline transport in the sea, favoring maritime transport beyond a certain distance. Depending on the storage location, one technology may be preferred to another. In the case of shipping, research (Roussanaly et al., 2021;

* Corresponding author.
E-mail address: guy.deweireld@umons.ac.be (G. De Weireld).

https://doi.org/10.1016/j.ccst.2024.100280
Received 29 June 2024; Received in revised form 16 August 2024; Accepted 18 August 2024

Phillips et al., 2022) has explored the optimal transport pressure by examining practices used for LNG (Liquefied Natural Gas). CO_2 transport by ship proves advantageous at pressures of 7 or 15 barg. The optimum pressure will depend on the size and the type of the cargo vessel, with a tendency for larger capacity vessels to transport at pressures below 7 barg.

In Western Europe, carbon capture and storage (CCS) sites are envisioned to be primarily located offshore due to large capacity of storage and the social acceptance by the public (Oei and Mendelevitch, 2013). Consequently, the transportation of CO_2 will play a key role in this entire process, with efforts focused on optimizing this crucial component of the chain.

For example, in Belgium, operator of gas transmission network (Fluxys) will provide a pipeline grid to cover areas where high CO_2 emissions plants are located (Belgium, 2022). Part of the pipelines will be a conversion of a natural gas grid. Continuous interconnections between France, Germany and the Netherlands are possible. In addition, the ports of Ghent (Remy et al., 2022), Antwerp and Zeebrugge will have temporary storage sites to keep the CO_2 liquefied for ship transportation.

As the CO_2 to be liquefied comes from different sources, it could contain different kinds of impurities in various concentrations. These impurities found in concentrated CO_2 are due to two factors. The first one is linked to the industrial process emitting the flue gas and the gas treatments already in application. The second factor is the type of capture unit and its operating performance. Several research have studied their effects on physicochemical properties such as density, viscosity, and vapor-liquid phase envelope change (Daud, 2021; Li et al., 2009; Wetenhall et al., 2014; Martynov et al., 2016). These impurities are linked to an increase in power consumption during compression but also involve possible corrosion or cavitation problems.

As impurities in CO_2 are problematic, gas transmission system operators are proposing specifications for CO_2. Pipeline transport is commonly restricted to concentrations beyond 95 mol% for CO_2 (de Visser et al., 2008; Anon., Fluxys 2022), with stringent limits imposed on certain compounds such as SOx, NOx, as well as water and oxygen to mitigate potential corrosion issues. Northern Light (Anon., Equinor 2019; Anon., Northern Lights 2024) advocates for high-quality CO_2 transport by ship, with even lower content thresholds than those required for pipeline transportation (Phillips et al., 2022).

Among the various articles in the literature, some authors have proposed an installation for purifying CO_2. Deng et al. (Deng et al., 2019) suggest a two-flash system with pressure variation to remove impurities from liquid CO_2. Gong et al. (Gong et al., 2022) further enhance this approach by adding a stripping column at the end of the chain to purify the liquid CO_2.

Two ways to liquefy CO_2 are available. The first involves leveraging the significant Joule-Thompson coefficient of CO_2 (1 K/bar at 303 K). The CO_2 is pressurized to reach the minimum pressure required for liquefaction with the cooling water. Liquid CO_2 is expanded to the desired pressure generating a vapor-liquid equilibrium. Vapor is recycled to be recompressed. This cycle is known as the Linde-Hampson or CO_2-open cycle (Fig. 1(a)). The second method employs a refrigeration machine to provide the necessary cold duty for liquefying CO_2 at the chosen pressure (Fig. 1(b)). The liquefaction machine is the classic process with refrigerant that is compressed up to the high pressure. This pressure depends on the outlet cooling water temperature used to liquefy the refrigerant through the heat exchanger before its expansion to generate vapor-liquid equilibrium. The refrigerant is expanded to the pressure corresponding to the temperature necessary to cool and liquefy the CO_2. The flow rate of the cycle is related to the total amount of cooling required to generate steam at the outlet of the heat exchanger, which then enters the compressor to close the loop. The operating conditions (pressure and temperature) in these cycles are dependent on the properties of the cooling water system and the heat exchangers, such as the inlet temperature, the temperature rise, and the pinch of the exchanger associated with its performance.

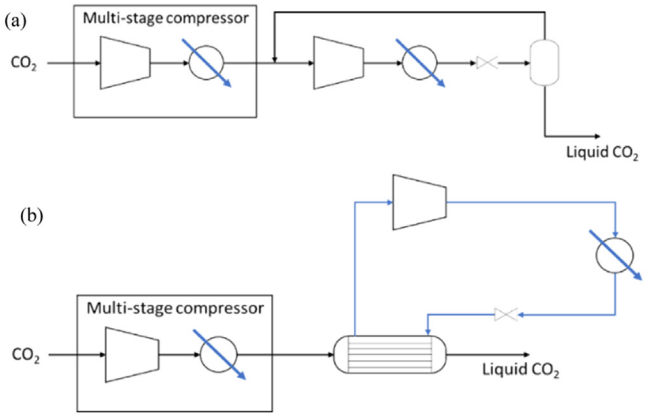

Fig. 1. (a) CO_2-open and (b) closed cycle liquefaction.

Research on CO_2 liquefaction primarily focuses on reducing the electrical consumption by optimizing the process. In the case of refrigeration machines, studies involve modifications such as adding compression-expansion stages, implementing cascade systems, or altering the refrigerant fluid (Jackson and Brodal, 2019; Seo et al., 2015; Seo et al., 2016; Alabdulkarem et al., 2012). For CO_2-open cycles, optimization is achieved through multi-stage expansions and the optimization of heat exchangers (Jackson and Brodal, 2019; Lee et al., 2012). Some articles also propose a hybrid process combining the Linde-Hampson cycle and a refrigeration machine (Seo et al., 2015; Chen and Morosuk, 2021).

Studies consistently indicate that 3-stage cycles are most energy-efficient for both methods (Jackson and Brodal, 2019; Seo et al., 2015; Seo et al., 2016; Lee et al., 2012). Ammonia and propane as a refrigerant fluid appears to be the most promising, whether for CO_2 liquefaction at 7 bar or 15 bar (Jackson and Brodal, 2019; Seo et al., 2015; Seo et al., 2016; Alabdulkarem et al., 2012; Chen and Morosuk, 2021). The choice between refrigeration machines and CO_2-open cycles depends on cooling water temperatures, favoring the open cycle at lower temperatures (Jackson and Brodal, 2019).

Among the various articles in the literature, only one author (Engel and Kather, 2018; Engel and Kather, 2017) addresses the case of CO_2 coming from a pipeline. However, research on transportation indicates that this type of liquefaction will be necessary.

The main objectives of the work are to explore the intricacies of CO_2 liquefaction processes, considering constraints and assumptions for transportation that significantly influence system behavior. While the usual choice for onshore CO_2 transport is transportation in supercritical state by pipelines, the reconditioning of existing pipelines introduces a distinctive challenge. In such cases, CO_2 is not conditioned into a supercritical state, and instead, it is transported as a gas within the maximum pressure limits set by the existing pipeline infrastructure (e.g. 30–35 bar).

This study examines a range of pressures including critical pressure for transition phase. A key variable in this analysis is the impurities content within CO_2, influenced by the emission source. These impurities significantly impact phase equilibrium, consumption rates, and the necessary purification steps for CO_2 transport via ships.

Table 1 presents the typical specifications for a pipeline transport in gas phase and a ship. Permanent gases such as CO, H_2, or O_2 may require liquid distillation to meet the specified standards. SOx, H_2S, and NH_3 are not included in the table as the pipeline specifications are equal to or lower than those set for the ship transportation. In this study, one of the key points of interest is the non-condensable gases, which result in higher consumption and CO_2 losses associated with purge streams.

At the end, the objective is to compare the 3-stage optimized system with various possible refrigerants (ammonia and propane), an

Table 1
Pipeline and ship CO_2 specification.

Component	Unit	Pipeline Fluxys (Fluxys 2022)	Ship Northern Lights (Northern Lights 2024)
CO_2	% mol	> 95	> 99.81 (Balance)
H_2O	ppm mol	< 40	≤ 30
H_2	ppm mol	< 7500	≤ 50
N_2	ppm mol	< 24,000	≤ 50
Ar	ppm mol	< 4000	≤ 100
CH_4	ppm mol	< 10,000	≤ 100
CO	ppm mol	< 750	≤ 100
O_2	ppm mol	< 40	≤ 10

optimized open CO_2 cycle, and a hybrid system of both processes for gaseous and supercritical CO_2, as well as CO_2 with specifications for pipeline transport, aiming to meet the requirements of transportation by ship. An investigation of the influence of cooling water temperature is also presented.

2. Details and design of the process

Considering the diverse sources of CO_2, the study incorporates multiple streams with varying levels of impurity. Cooling water temperatures, determined by industrial locations, are used as dynamic parameters capable of modifying optimal cycle sequences.

This research is complemented by the study of various liquefaction systems. The first one is a 3-stage closed cycle optimized by Engel & Kather (Engel and Kather, 2018) as the most efficient closed cycle studied for supercritical CO_2. In the present work, two new processes are also investigated. The second is a multi-stage open cycle, and the last one is a hybrid system between the two previous cycles. Two refrigerants were considered in the closed cycle. By systematically varying input parameters, the study aims to identify the most optimal scenarios to specific cases. The main goal is to offer insights into the complexities of CO_2 transport, providing valuable knowledge to inform and optimize the practical aspects of this critical component in the pursuit of sustainable and efficient energy solutions. Table 2 summarizes the different variable study in this work.

The various cases of liquefied CO_2 are chosen to establish a benchmark, which is pure CO_2, for comparing different technologies. The case with only nitrogen allows studying the system's reaction with an impurity that is relatively common in capture techniques. Finally, the case with the maximum impurities allowed from a pipeline reflects the concentrations listed in the Table 1. In this work flue gas is considered as dry before process. Indeed, 40 ppm of water corresponds to a dew point of approximately −26 °C, which is too high and would result in ice formation in the process. Furthermore, since water is much less volatile than CO_2, it remains in the liquid phase preventing the required purity for transport by ship from being reached.

The impurities present in CO_2 have an influence on its thermodynamic and physicochemical properties compared to pure CO_2. The Fig. 2 shows the vapor-liquid equilibrium for the different cases studied. It can be observed that pure CO_2 is liquid at −28 °C for a minimal pressure of 15 bar. However, at the same temperature, the liquefaction pressures for the other two cases are approximately 26 bar and 44 bar. This is particularly evident when comparing pure CO_2 to CO_2 with impurities, as the last one required higher pressure at fixed temperature or lower temperature respectively at fixed pressure. Therefore, it is necessary to purify the CO_2 to achieve complete liquefaction.

Table 2
Data studied in the work.

Variables	Data set
Cooling water temperature	From 5 to 35 °C
Inlet pipeline pressure	From 25 to 65 bar
Outlet liquid CO_2 pressure	15 bar
Gas to liquefy	Pure CO_2
	CO_2 with 2 % N_2
	CO_2 with maximal gas pipeline impurities
Liquefaction units	3-stage open cycle
	3-stage closed cycle
	Hybrid cycle (2-stage closed cycle with 1-stage open cycle)
Refrigerant	Ammonia (R-717)
	Propane (R-290)

2.1. Process configurations

The 3-stage closed-cycle (Fig. 3), presented by Engel and Kather (Engel and Kather, 2018), is a refrigeration machine that cools and liquefies CO_2 using a refrigerant. The refrigerant is compressed in the R-C1 compressor to the liquefaction pressure associated with the temperature of the hot source (cooling water). The pressures of the second and the third stages are determined by the liquefaction temperature of the different CO_2 expander T3 and T4 respectively. For each stage, cooling water is used to chill compressed gas before entering in flash (R-F1 and R-F2). Flash generates saturated liquid used for the CO_2 liquefaction. In the presence of impurities, the phase change temperature along the heat exchanger must be considered the outlet temperature of the pinch in the exchanger. The vapor is superheated before entering the compressor to prevent any liquid carryover into it. A flash unit is placed at the end of the chain to treat impurities in the liquid CO_2. Turbines are employed to generate electricity during the expansion of CO_2.

The open cycle (Fig. 4) uses the Joule-Thompson coefficient of CO_2 for self-refrigeration. Liquid CO_2 is expanded trough turbines (T2, T3, T4) generating vapor-liquid equilibrium at lower pressure and lower temperature. Following expansion, the saturated vapor is directly sent to a compressor (C1, C2, C3) to recompress CO_2 to the pre-expansion pressure. The pressure at the first expansion (T1) is linked to the temperature of the cooling water, which facilitates the liquefaction of CO_2 at the main heat exchanger (HX1). Engel and Kather (Engel and Kather, 2017) address a mass balance issue in an open cycle with impurities. To overcome this problem and handle a flush with impurities, a flash (F1, F2, F3) is introduced at the outlet of turbine to purge the gas that has not been liquefied, without adding a prior purification step.

The hybrid cycle (Fig. 5) is a combination of the closed-cycle and open-cycles. The 2-stage closed cycle allows the liquefaction of CO_2 at an intermediate pressure before expanding liquid CO_2 to the transport pressure, generating both the liquid phase (the final product) and a vapor phase. The vapor phase is recompressed and sent back before the heat exchanger, where CO_2 is liquefied in conjunction with the refrigeration cycle. A purge is added at the liquefaction outlet to extract impurities from the CO_2 in the pipeline.

For these different cycles, the pressure at outlet of the first turbine (T1) is set to produce a saturated liquid stream. The last turbine (T4) determines the outlet pressure. The intermediate turbine pressures (T2 and T3) are optimized to minimize the total electrical consumption of the process. This optimization is performed using the integrated optimization tool in Aspen Plus®. In the case where CO_2 from the pipeline is in a gaseous state, the first turbine is removed. In the open cycle, CO_2 enters the system before compressor C1 if the pressure is below the liquefaction pression of CO_2 with the cooling water.

Since the permissible impurities in liquid CO_2 are very strict, distillation of the CO_2 may be necessary to purify it for transportation. An advanced process including a distillation column (Fig. 6) is suggested for one of the cycles (hybrid cycle in this case). The column is fed by the stream coming from turbine T3 and the recycle from compressor C1. This stream is in a vapor-liquid state. The distillation column is modeled using the RadFrac block in Aspen Plus® in rate-based mode. A structured packing, the Mellapack 250Y, is considered as internal in the contactor. The condensation is partial, and condenser is fed by the last stage of the refrigeration unit (HX4). The vapor stream (stream 11) corresponds to the process purge. The liquid is returned to the column as reflux.

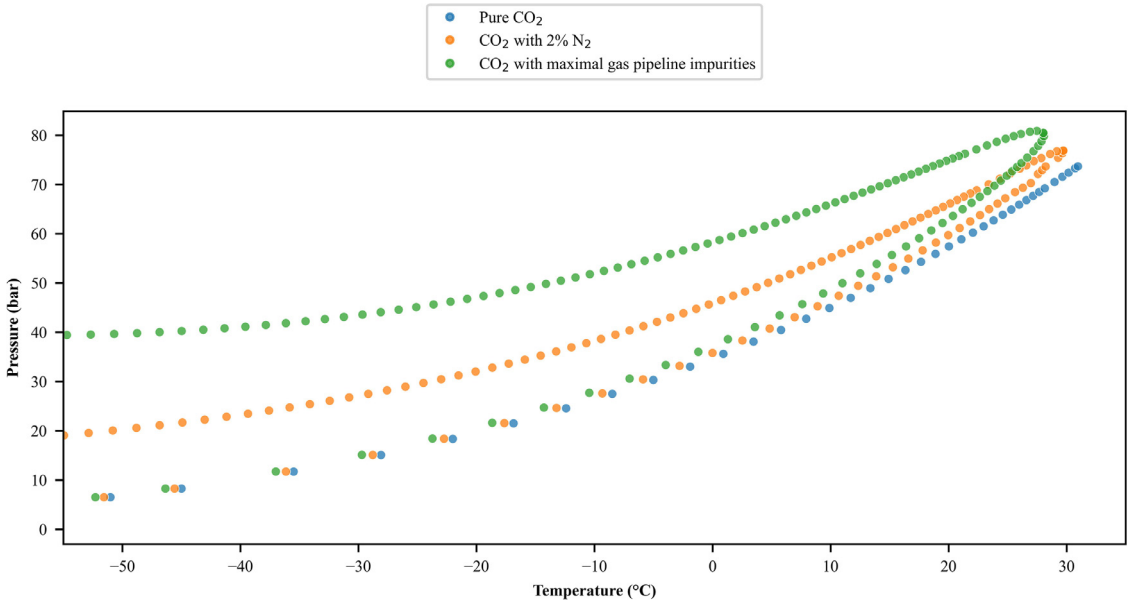

Fig. 2. Vapor-liquid equilibrium for the different studied cases.

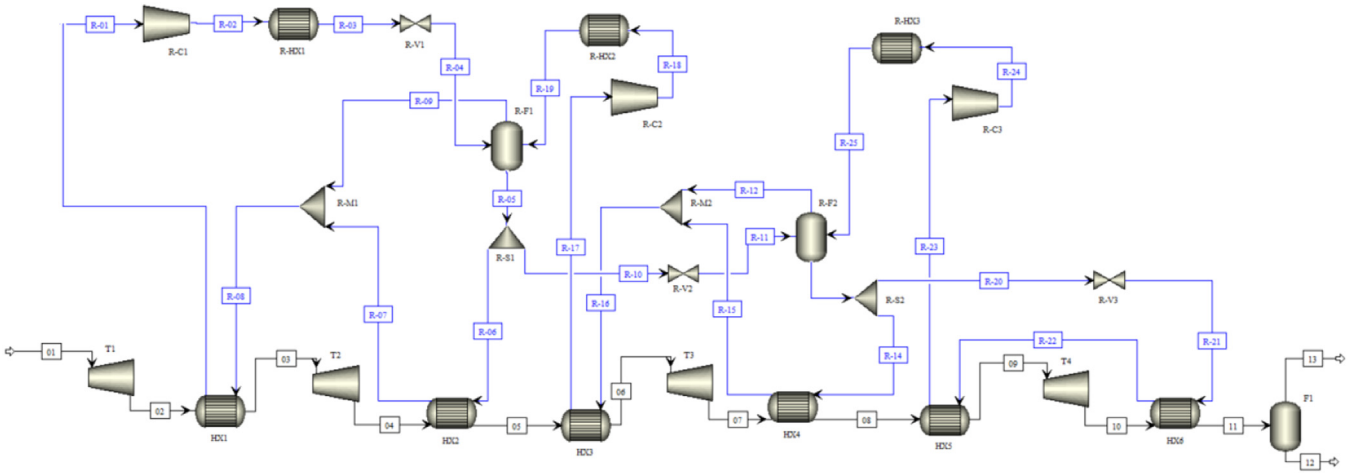

Fig. 3. 3-stage closed cycle.

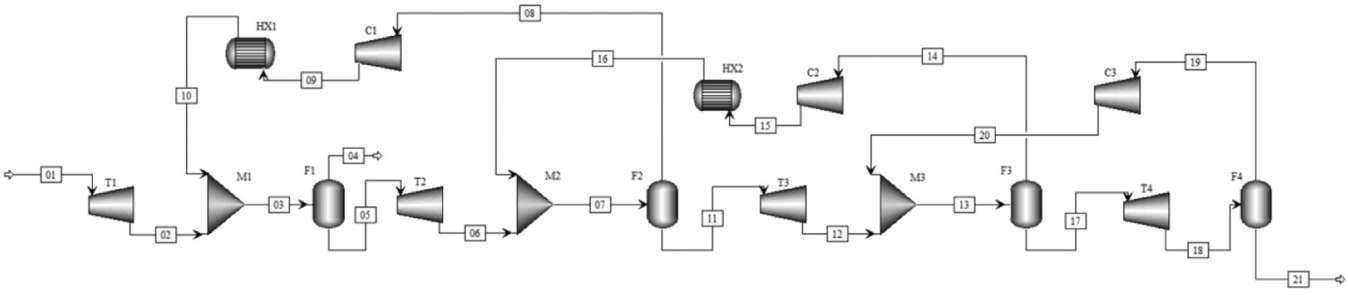

Fig. 4. 3-stage open cycle.

Water is used as the energy input for the reboiler. The liquid fraction recovered from the reboiler is sent to turbine T4 to be expanded to the transport pressure. The column introduces additional variables to the global process. These include the feed stage, packing height, and boil up ratio, which is the ratio of vapor flow rate from the bottom stage to the liquid bottom product rate. The pressure in the column is defined by the pressure of turbine T3 and the temperature of the condenser by heat exchanger HX4.

The modelling of the process is done in Aspen Plus® V14 software. Peng-Robinson with Boston-Mathias modification equations of state (Mathias and Copeman, 1983) was used to determine thermodynamics properties of CO_2 stream with and without impurities (Engel and Kather, 2017; Mazzoccoli et al., 2012; Zhang et al., 2006). NIST Reference Fluid Thermodynamic and Transport Properties Database (REFPROP) for the closed cycle (Huber et al., 2022). Helmholtz equation of state for ammonia developed by Goa et al. (Gao et al., 2023) is used for R-717 properties and the thermodynamics properties for propane developed by Lemmon et al. (Lemmon et al., 2009) is used for R-290.

Table 3 lists the different assumptions taken for the modelling of the Aspen Plus® model.

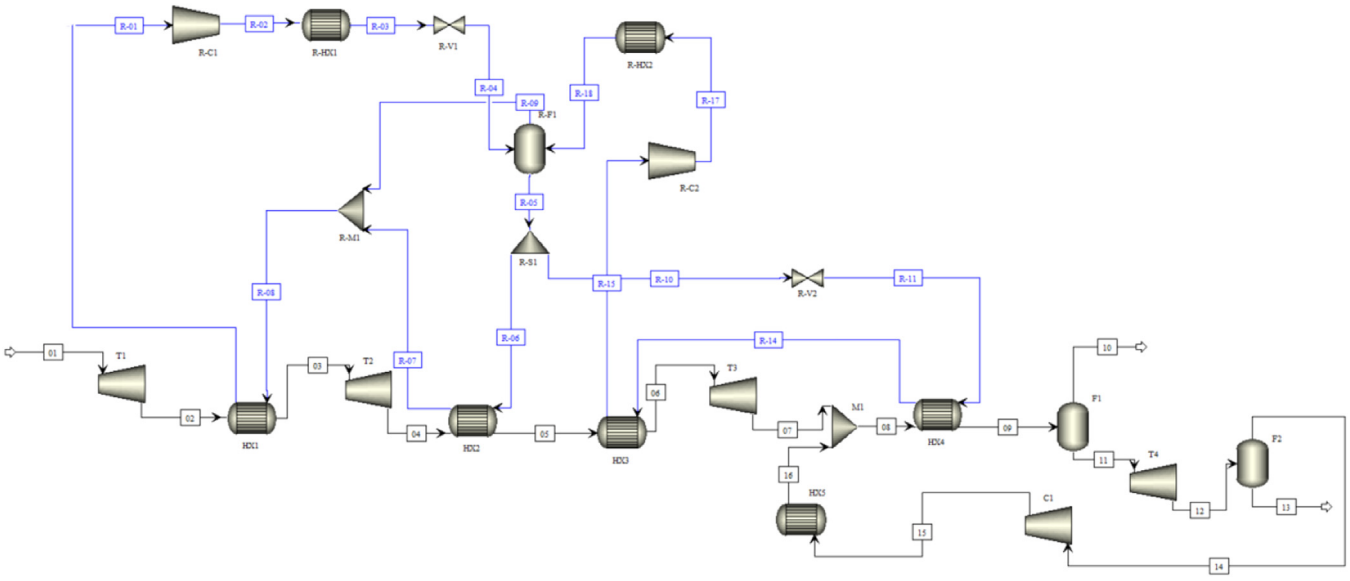

Fig. 5. Hybrid cycle (2-stage closed cycle with 1-stage open cycle).

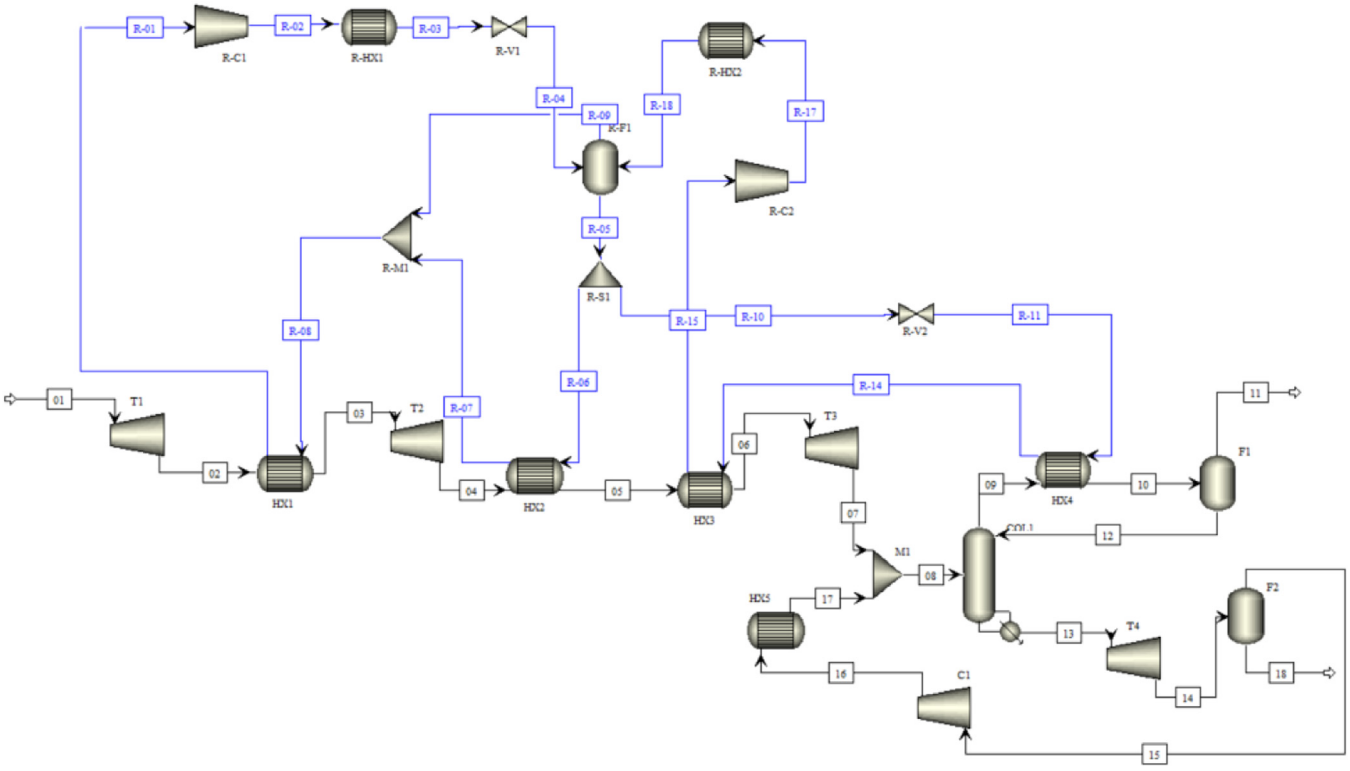

Fig. 6. Hybrid cycle including a distillation column.

Table 3
Assumption for the simulations (*phase change assimilate to liquid).

Assumptions	Value	Reference
Gas – liquid heat exchanger pinch	10 °C	(Costa et al., 2024a)
Liquid – liquid* heat exchanger pinch	3 °C	(Engel and Kather, 2017)
Superheat at compressor inlet	5 °C	(Engel and Kather, 2017)
Isentropic compressor efficiency	85 %	(Deng et al., 2019; Engel and Kather, 2017)
Isentropic dense phase expander efficiency	90 %	(Engel and Kather, 2017)
Isentropic biphasic expander efficiency	70 %	(Engel and Kather, 2017)
Inlet cooling water temperature (base case)	15 °C	–
Cooling water temperature rise	1 to 10 °C	–
Inlet pipeline temperature	20 °C	–
Inlet flowrate	100 t/h	–

Table 4
Capital cost variable of components (*: $F_p = 1$ for $P < 5$ barg).

Equipment Type	K_1	K_2	K_3	B_1	B_2	F_{BM}	C_1	C_2	C_3
Compressors Centrifugal	2.2897	1.3604	−0.1027	–	–	2.7	–	–	–
Floating head HX	4.8306	−0.8509	0.3187	1.63	1.66*	–	0.03881	−0.11272	0.08183
Turbines	2.2476	1.4965	−0.1618	–	–	1	–	–	–
Vertical towers and vessels	3.4974	0.4485	0.1074	2.25	1.82	–	–	–	–

The cooling water temperature rise is a parameter that is often neglected and fixed. However, it influences the outlet temperature of the cooling water, which is directly related to the liquefaction temperature of the refrigerant fluid (closed and hybrid cycles) and CO_2 (open cycle). When its value is increased, the flow rate of cooling water decreases, reducing the load on cooling towers or air condensers, but the liquefaction pressure increases, resulting in greater compressor consumption.

In the presence of impurities, vapor-liquid equilibria appear between the compounds, resulting in a loss of CO_2 in the purge streams that reject most of the non-condensable gases. In this study, this loss is quantified by the final recovery rate of the liquefaction process:

$$Recovery = \frac{m_{CO_2\ out}}{m_{CO_2\ in}} \tag{1}$$

where m_{CO_2} is the CO_2 mass flowrate (t_{CO2}/h) at inlet (*in*) and outlet (*out*) of the liquefaction unit.

2.2. Energy analysis

The analysis of energy, in accordance with the first law of thermodynamics, primarily examines the energy quantity associated with a process, disregarding losses. The Key Performance Indicator (KPI) commonly employed to demonstrate system efficiency is the electrical consumption per ton of CO_2. In a liquefaction unit, the predominant energy requirement arises from electrical consumption, mainly driven by the compressors. Turbines give negative electrical consumption as a generation of electricity.

$$E_{consumption} = \frac{W_C + W_T}{m_{CO_2\ out}} \tag{2}$$

where $E_{consumption}$ is the electrical consumption of the process (kWh/t_{CO2}), W_C is the compressor mechanical power rate (kW), W_T is the turbine mechanical power rate (kW).

2.3. Economic analysis

The methodology for calculating Capital Expenditures (CAPEX) and Operational Expenditures (OPEX) of a process is based on (Turton et al., 2018). The Chemical Engineering Plant Cost Index (CEPCI) serves as an indicator to account for inflation in equipment and services costs related to the chemical process industries. The following formula, derived from the CEPCI, is employed for adjusting the actual cost (C_{actual}) to a reference year ($C_{reference}$):

$$C_{actual} = C_{reference}\left(\frac{I_{actual}}{I_{reference}}\right) \tag{3}$$

where C represents the cost (€), and I is the index (-) with the subscripts 'actual' and 'reference' indicating their respective values. Costs are computed using the CEPCI of 2022, valued at 816.2 (Maxwell, 2022).

Economic analysis involves estimating CAPEX, which is calculated based on purchased equipment cost (C_p^0), bare module cost (C_{BM}) encompassing direct and indirect costs, contingency costs, and fees. Eqs. (4)-(7) are utilized for CAPEX calculation, with parameters detailed in Table 4.

$$\log_{10}C_p^0 = K_1 + K_2\log_{10}(S) + K_3[\log_{10}(S)]^2 \tag{4}$$

Table 5
Base case assumptions for OPEX.

Parameter	Value
Utility Cost (C_{UT})	Electricity: 100 €/MWh Cooling water: 0.3 €/m^3
Operating Labor Cost (C_{OL})	54,000 €/labor/year (Chauvy et al., 2020)
Direct supervisory and clerical labor	0.18 C_{OL}
Maintenance and repairs	0.06 CAPEX
Operating supplies	0.15 (0.06 CAPEX)
Laboratory charges	0.15 C_{OL}
Patents and royalties	0.03 OPEX
Local taxes and insurance	0.032 CAPEX
Plant overhead costs	0.6 (1.18 C_{OL} + 0.06 CAPEX)
Administration costs	0.15 (1.18 C_{OL} + 0.06 CAPEX)
Distribution and selling costs	0.11 OPEX
Research and development	0.05 OPEX

$$C_{BM} = C_p^0\left[B_1 + B_2\ F_P\ F_M\right] = C_p^0\ F_{BM} \tag{5}$$

$$\log_{10}F_{p,hx} = C_1 + C_2\ \log_{10}(P) + C_3\ [\log_{10}(P)]^2 \tag{6}$$

$$F_{p,vessel} = \frac{\frac{P\ D}{2\ St\ E - 1.2\ P} + CA}{t_{min}} \tag{7}$$

where C_p^0 represents the purchased equipment cost at ambient operating pressure using carbon steel construction, S is the size of the equipment, F_M is the material factor (assumed as 1 for carbon steel), F_P is the pressure factor, P is the pressure (bar), D is the diameter (m), t_{min} is the minimum allowable vessel thickness ($6{,}3.10^{-3}$ m), CA is the corrosion allowance ($3{,}15.10^{-3}$ m), E is the weld efficiency (0.9), St is the allowable stress for carbon steel (944 bar) and B_i, C_i and K_i are constants.

For the distillation column using Mellapack 250Y, the costs for packing, distributor, distributor support, chimney tray collector, and packing support grid and auxiliaries (cladding, distributor, connections, ladders, platforms and handrails, etc.) are calculate with Wang et al. (Wang et al., 2015) correlations.

The contingency cost is subject to variation based on the reliability of cost data and the completeness of the available process flowsheet. It serves as a safeguard against oversights and inaccurate information and is integrated into the cost assessment. Unless specified otherwise, contingency costs and fees are assumed to be 15 % and 3 % of the bare module cost, respectively. The summation of these costs with the bare module cost yields the total module cost.

Operational Expenditures (OPEX) can be determined using a range of known or estimated costs outlined in Table 5. These costs encompass CAPEX, operating labor cost, and utility cost.

The OPEX is expressed by the equation:

$$OPEX = 1.235\ (C_{UT}) + 2.735\ C_{OL} + 0.180\ CAPEX \tag{8}$$

Given that the CAPEX represents the overall plant cost, it is spread out over the plant's lifespan, typically considered as 25 years. Finally, the CAPEX is annualized by factoring with an inflation rate using the following equation:

$$CAPEX_a = CAPEX\frac{i(1+i)^n}{(1+i)^n - 1} \tag{9}$$

where $CAPEX_a$ denotes the annuity cost (€), i is the inflation rate (6.5%) (Chauvy et al., 2020) and n is the number of years of annuity interest.

The KPI for the economic analysis is the $Capture\ cost$ defined by the sum of the annuity of CAPEX and OPEX:

$$Capture\ cost\left(\Delta/t_{CO_2}\right) = \left(CAPEX_a + OPEX\right)/\dot{m}_{CO_2}out \tag{10}$$

2.4. Exergy analysis

Exergy is defined as the maximum useful work obtainable when a system interacts with a reference environment. It characterizes the quality of energy within a system and serves as a valuable metric for quantifying inefficiencies and losses. In this study, exergy analysis is conducted following the principles outlined by Szargut (Szargut, 1989).

The analysis begins with defining the system boundaries, which encompass all relevant components involved in CO_2 transport facilities. This approach ensures that all significant factors impacting the exergy performance are considered.

The exergy (Eq. (11)) of each stream within the system is calculated using the fundamental thermodynamic relationships, taking into account physical and chemical exergy terms, while neglecting kinetic and potential exergy terms. These calculations are performed relative to a reference environment (P_0 (1 atm) and T_0 (25 °C) with relative humidity of 70 %), established to determine the exergy values of the system components under standard environmental conditions. The reference environment proposed by Rivero & Garfias (Rivero and Garfias, 2006) is considered to calculate the chemical exergy of the different molecules.

$$ex = ex_{ph} + ex_{ch} \tag{11}$$

$$ex_{ph} = \left(h - h_0\right) - T_0\left(s - s_0\right) \tag{12}$$

$$ex_{ch} = \sum_i y_i\left(ex_{ch,i} + RT_0 lny_i\right) \tag{13}$$

where ex is the exergy (kJ/mol), ex_{ph} is the physical exergy (kJ/mol), ex_{ch} is the chemical exergy (kJ/mol), T_0 is the environment temperature (K), s is the entropy (kJ/(mol.K)), subscript 0 is for environmental reference state, y_i is the gas composition, and i is the compound.

Exergy destruction (Ex_D) refers to the irreversible loss of exergy within a system due to inefficiencies or irreversibility during energy conversion processes. It represents the dissipation of exergy into forms that are no longer available to perform useful work, leading to reduced system efficiency and increased entropy generation. Essentially, the exergy is equal to the incoming and outgoing exergy of the system, supplemented by the exergy associated with heat transfer (Ex_Q) and work interactions (Ex_W). This expression includes the irreversible dissipation of exergy attributable to diverse processes and interactions within the system.

$$Ex_D = \sum n\ ex_{out} - \sum n\ ex_{in} + Ex_Q + Ex_W \tag{14}$$

$$Ex_Q = \sum \int_{T=T_{in}}^{T_{out}} \left(1 - \frac{T_0}{T}\right) dQ \tag{15}$$

$$Ex_W = \sum W \tag{16}$$

Where Ex_D is the exergy destruction (kW), Ex_Q is the heat transfer exergy (kW), Ex_W is the work exergy (kW) n is the mole flow rate (mol/s), subscript *in* an *out* are respectively for inlet and outlet, and T is the temperature of the heat source (K).

Furthermore, exergy efficiency (η_{ex}) as an interesting KPI to evaluate the effectiveness of CO_2 transport technologies. Exergy efficiency is calculated as the ratio of useful exergy output to the total exergy input, providing a quantitative measure of system performance (Costa et al., 2024a). In other words, it represents the exergy destruction and the exergy loss (Ex_L) associated to the exergy from by-products, discharged streams, or unutilized cooling water.

$$\eta_{ex} = \frac{Ex_{Out}}{Ex_{In}} = 1 - \frac{Ex_D + Ex_L}{Ex_{In}} \tag{17}$$

3. Results and discussions

Firstly, sensitivity study on cooling water temperature rise is carried out to define the value used in the rest of the work. The open and closed cycles are used to perform the analysis considering the following conditions: pure CO_2 at 25 bar using R-717 refrigerant with a temperature of cooling water at 15 °C.

Pure CO_2 was considered in the different liquefaction processes with the variation of cooling water temperature. The outlet pipeline pressures are set to be in the gaseous state. The KPIs are utilized to determine which process is more favorable under the given initial conditions.

The case of CO_2 with 2 mol% of N_2 and the Fluxys pipeline more stringent specification (Table 1) are also studied considering an inlet pressure of 25 bar. Following the results of pure CO_2, the refrigerant considered is also R-717, and the cooling water temperature is fixed at 15 °C.

3.1. Sensitivity study on cooling water temperature rise

A sensitivity study on the increase of the cooling water temperature was conducted to determine the optimal value from an economic standpoint. Considering the assumption of the cooling water price (0.3 € per m^3/h), there exists an optimum between a very low temperature increase, which implies a higher flow rate of cooling water, and a higher temperature increase, which results in a higher temperature in the refrigeration circuit to meet the imposed pinch between the two fluids.

Despite an increase in electrical consumption and thus operating expenses (OPEX), an optimum is observed at around 7 °C temperature increase for the liquefaction cost considering the closed cycle (Fig. 7(a)). However, within the range of 5 to 10 °C, the cost savings are at a maximum of 0.1 €/t_{CO2}. For the open cycle (Fig. 7(b)), the minimum liquefaction cost is around 5 °C temperature rise. The difference in comparison with closed cycle is that pressure to liquefy CO_2 with cooling water is close to the critical pressure. The increase in the rise of the cooling water temperature results in a higher liquefaction temperature, leading to a more significant increase in electrical consumption in the case of the open cycle. For the remainder of the study, a cooling water temperature rise of 7 °C will be considered for closed cycle and hybrid cycle and a rise of 5 °C for the open cycle.

3.2. Pure CO_2 case study

The different processes were simulated considering the various case studies mentioned earlier (Fig. 8). For the various case studies, the different cycles are very close to each other in terms of electrical consumption. However, for the lowest cooling water temperatures, the open cycle is the most interesting one, followed by the hybrid cycle. For cycles with refrigerants, ammonia is predominantly the most interesting one. For lower cooling water temperatures, ammonia and propane have very similar energy consumption (< 0.5 % difference). However, as the cooling water temperature increases, the difference becomes more significant, reaching up to 10 %. There is over a 100 % increase in electrical consumption between the minimum and maximum cooling water temperatures. Finally, there is a decrease in energy consumption due to CO_2 entering at a higher pressure in the liquefaction system. Pressurized CO_2 has a higher liquefaction temperature, allowing the first liquefaction stage to operate at a higher temperature, resulting in an energy gain in liquefaction.

Upon closer examination of the results for the hybrid cycle (Fig. 9), it can be noticed, as might be expected, that the liquefaction cost trends similarly to electrical consumption. For 25 bar, the cost range is between 6 and 11 €/t_{CO2}, and for 65 bar pressure, it ranges from 4 to 8 €/t_{CO2}. This cost may seem relatively low but is not negligible when considering the entire CCUS chain. Regarding exergy, there is a maximum at a cooling water temperature of 5 °C and a pressure of 55 bar. This maximum is related to the fact that, considering the temperature rise and the

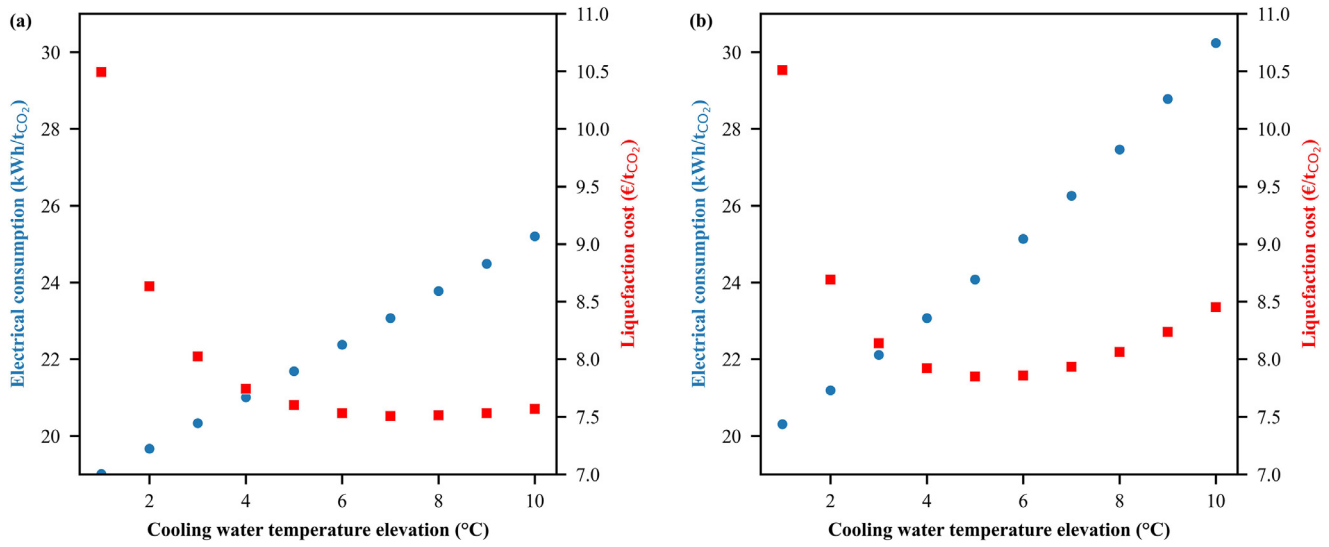

Fig. 7. Electrical consumption and liquefaction cost in function of the cooling water temperature rise for closed cycle (a) and open cycle (b).

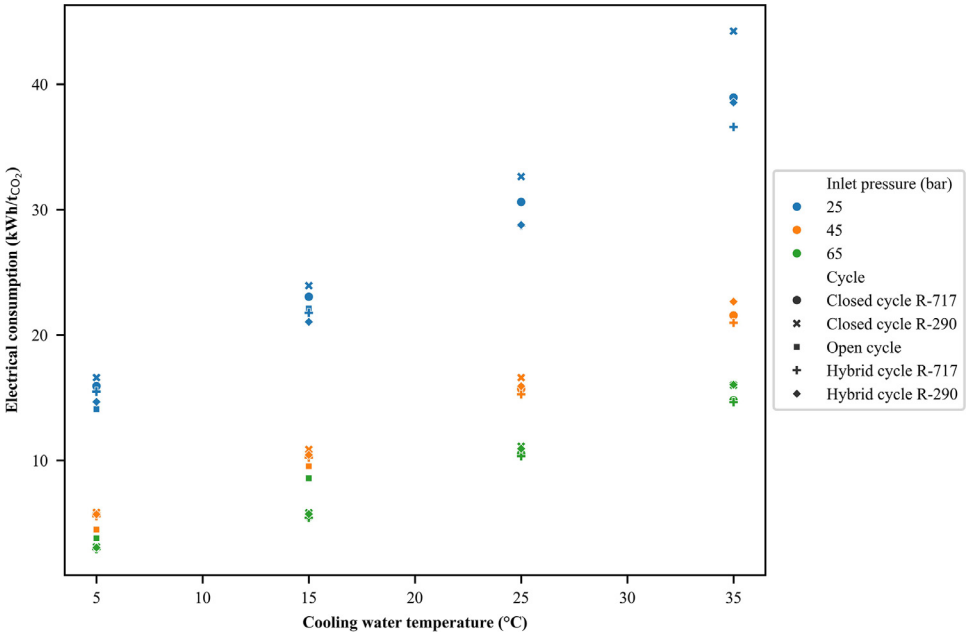

Fig. 8. Electrical consumption of the cycles in function of the inlet pressure, cooling water temperature and the refrigerant for pure CO_2.

pinch within the heat exchangers, this pressure is close to the CO_2 dew point. For the others, the exergy efficiency increases with higher inlet pressure.

3.2.1. *Electricity price impact on the liquefaction cost*

The impact of electricity prices on the liquefaction cost is a crucial aspect to consider in the optimization of liquefaction processes. Fluctuations in electricity prices can significantly influence operational expenses and ultimately affect the economic viability of CCUS chains.

To assess this impact, a sensitivity analysis was conducted, varying electricity prices within a realistic range from 50 to 250 €/MWh. The results (Fig. 10) indicate a direct correlation between electricity prices and liquefaction costs across all cycles studied. Higher electricity prices lead to increased operational expenses, resulting in higher liquefaction costs per ton of CO_2 liquefied. Relative to the base case at 100 €/MWh, the liquefaction cost for the hybrid process exhibits a variation ranging from −15 % to +40 % for the two extremes considered for the electricity price. It can also be noticed that the closed cycle closely approaches the hybrid cycle as the electricity price decreases.

These findings underscore the importance of considering electricity price dynamics in the design and operation of liquefaction facilities. Strategies such as demand-side management, renewable energy integration, and energy storage solutions may offer avenues for mitigating the impact of electricity price volatility on liquefaction costs, thereby enhancing the economic feasibility of these technologies.

3.2.2. *Sensitivity analysis on simulation assumptions*

To evaluate the impact of the various assumptions outlined (see Table 3) on the simulation, a sensitivity analysis of these assumptions on electrical consumption was conducted. The baseline scenario involves a closed-loop system using R-717, with pure CO_2 entering at a pressure of 25 bar and water cooling at 15 °C. As observed in Table 6, the parameter with the most significant impact on electrical consumption is the pinch at the liquid-liquid heat exchangers. This type of exchangers is used as the evaporators and condensers of the refrigeration system. A smaller pinch point leads to a higher boiling temperature and a lower condensation temperature, which respectively result in a higher low-side pressure and a lower high-side pressure, thereby reducing the sys-

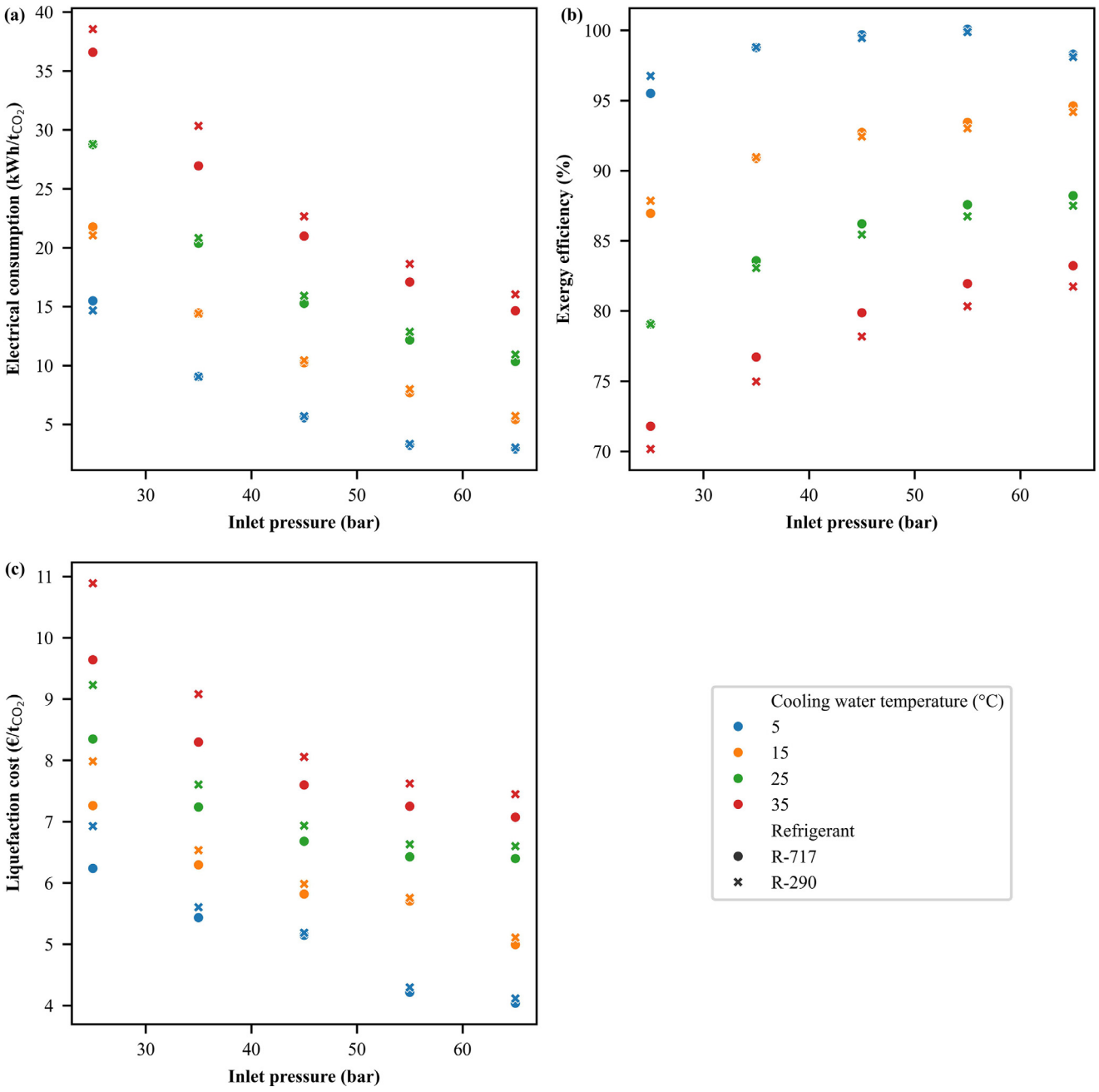

Fig. 9. Electrical consumption (a), exergy efficiency (b), and liquefaction cost (c) for hybrid cycle in function of the inlet pressure, the refrigerant, and the cooling water temperature.

Table 6
Electrical consumption variation of the different simulation assumptions.

Gas – liquid heat exchanger pinch	Superheat at compressor inlet	Liquid – liquid* heat exchanger pinch	Isentropic compressor efficiency	Isentropic biphasic expander efficiency	Electrical consumption (kWt/t_{CO_2})	Variation (%)
3	5	10	0.85	0.70	22.7	0.0
3	5	10	0.80	0.70	24.2	6.3
3	5	10	0.90	0.70	21.4	−5.6
3	5	10	0.85	0.65	22.7	−0.1
3	5	10	0.85	0.75	22.7	0.1
5	5	10	0.85	0.70	25.7	13.2
1	5	10	0.85	0.70	19.8	−12.6
3	2	10	0.85	0.70	22.4	−1.5
3	8	10	0.85	0.70	23.0	1.3
3	5	5	0.85	0.70	22.7	−0.2
3	5	15	0.85	0.70	22.7	0.0

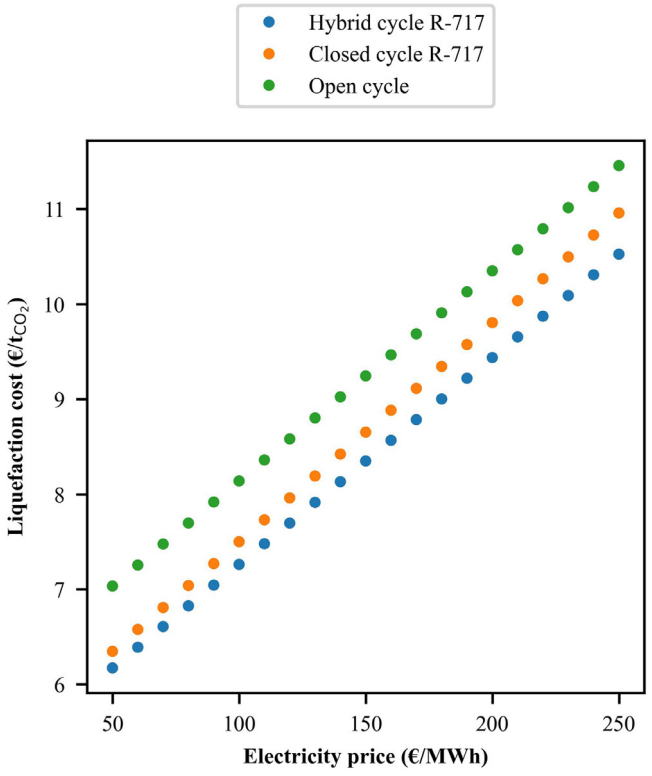

Fig. 10. Impact of the electricity price variation on liquefaction cost for several cycle.

tem's compression ratio. The second most influential parameter is the isentropic efficiency of the compressors, with a variation of 5 to 6 % compared to the baseline scenario for a 5 % change of the isentropic compressor efficiency. Efficiency directly affects the power consumption of the compressors.

3.3. CO_2 with impurities case studies

The impurities contained in the CO_2 modify the dew point of the fluid, requiring more significant refrigeration of the fluid to achieve sufficient CO_2 liquefaction. However, the triple point of CO_2 is at −56.6 °C. The formation of dry ice inside a heat exchanger would seriously damage it. Therefore, a limit of −54 °C is set to ensure that no dry ice forms in the process. In the closed cycle, the liquefaction temperature of heat exchanger HX6 is varied to obtain liquid CO_2 while reducing the amount of CO_2 leaving with the non-condensable gases. In the open cycle, the variable is the pressure of compressor C1, which allows for complete liquefaction of the stream with the cooling water. Finally, in the hybrid cycle, both pressure and temperature are variables that are adjusted respectively at turbine T3 and heat exchanger HX4, providing an additional degree of freedom compared to the two previous processes.

3.3.1. Case 1: CO_2 flow containing 2 % of N_2

The results of the closed cycle considering a variation of liquefaction temperature (Fig. 11) show a decrease in energy consumption directly related to the installation cost. The recovery, expressing the inverse of CO_2 loss, decreases with increasing temperature while remaining significantly high (>98 %). Exergy efficiency exhibits a maximum at −52 °C, corresponding to the optimal utilization of energy relative to the amount of recovered and liquefied CO_2.

Fig. 12 demonstrates the outcomes of the open cycle concerning escalating compressor pressure ranging from 64 to 82 bar before undergoing liquefaction via cooling water. As the compressor pressure rises, both electrical consumption and liquefaction cost exhibit a minimum. These minima occur at 70 and 72 bar, respectively. They are closely tied to the overall process recovery, which escalates with pressure but encounters difficulty in attaining the 90 % mark. This variance in recovery compared to the closed cycle is attributed to the interplay of interactions between nitrogen and carbon dioxide. In this scenario, the liquefaction temperature rises, and despite the heightened compression, the vapor mixture contains a greater concentration of CO_2 than in a colder mixture. In terms of exergy efficiency, the peak is reached at 78 bar with an approximate recovery rate of 85 %.

The outcomes from the hybrid cycle analysis (Fig. 13) indicate a correlation between consumption and recovery rate. Specifically, an increase in recovery is accompanied by an increase in consumption. When pressure is varied at a constant temperature, there's a slight increase in electrical consumption but a notable enhancement in recovery. Conversely, raising the temperature results in both higher electrical consumption and increased recovery. Notably, at a temperature of −48 °C, exergy efficiency reaches its peak for a pressure of 18 bar, with the optimum efficiency attained at a recovery rate of 99.25 % for an electrical consumption of 47.1 kWh/t_{CO2}.

The findings from the preceding analyses underscore that both the closed cycle and the hybrid cycle stand out as the most promising approaches for mitigating CO_2 losses in purge streams. The hybrid cycle not only exhibits slightly lower energy consumption compared to the closed cycle across various instances of pure CO_2, but also demonstrates superior performance in scenarios involving CO_2 with impurities. Moreover, in cases where the outlet CO_2 pressure is constrained to 7 bar to prevent dry ice formation, there exists a remarkably narrow temperature range (−54 to −50 °C), due to liquefaction temperature of CO_2 at this pressure. However, the introduction of a second degree of freedom through variations in liquefaction pressure enables the manipulation of variables, thereby widening the maneuvering zone. This facilitates the reduction of consumption while simultaneously ensuring effective management of CO_2 losses.

Nevertheless, the simulations were conducted as for pure CO_2, considering complete liquefaction for the intermediate stage of both the closed and hybrid cycles. To increase the degrees of freedom in the process, heat exchangers HX2 for both cycles and HX4 for the closed cycle were added to the variables of the objective function, minimizing the electrical consumption of the process.

The results from the optimized hybrid cycle (Fig. 14), where partial liquefaction takes place at the intermediate stage in the HX2 heat exchanger, consistently demonstrate lower consumption and consequently higher exergy efficiency compared to scenarios where the stream undergoes complete liquefaction at the intermediate stage. In this instance, the optimal exergetic point (−48 °C and 18 bar) stands at 33.5 kWh/t_{CO2}, representing nearly a 30 % reduction of energy consumption compared to full liquefaction at the intermediate stage. The liquid fraction fluctuates between 75 % and 90 %, with a tendency to increase at lower fixed temperatures for the last stage liquefaction. Pressure exerts a minimal influence on the variation of this intermediate liquid fraction. Notably, the maximum exergy efficiency is altered and peaks at 79.65 % in this scenario, occurring at −38 °C and 18 bar. At this stage, the recovery rate reaches 97.60 %, accompanied by a cost of 8.63 €/t_{CO2}, which corresponds to a consumption rate of 28.9 kWh/t_{CO2}.

3.3.2. Case 2: CO_2 flow containing maximal gas pipeline impurities

This scenario corresponds to the most stringent specifications acceptable, expected water, in the pipeline resumed in Table 1. Comparing the results obtained with CO_2 with 2 % nitrogen for the hybrid cycle, a slight overall increase in consumption can be observed (Fig. 15). The maximum exergy efficiency is 74.8 % and occurs at −40 °C and 20 bar. The liquefaction cost for this point is 9.35 €/t_{CO2} for a consumption of 32.5 kWh/t_{CO2} with a recovery of 95.5 %. Compared to 2 % nitrogen, the recovery is lower by 2 %, but overall, the price per ton of CO_2 is slightly increased with 0.7 €.

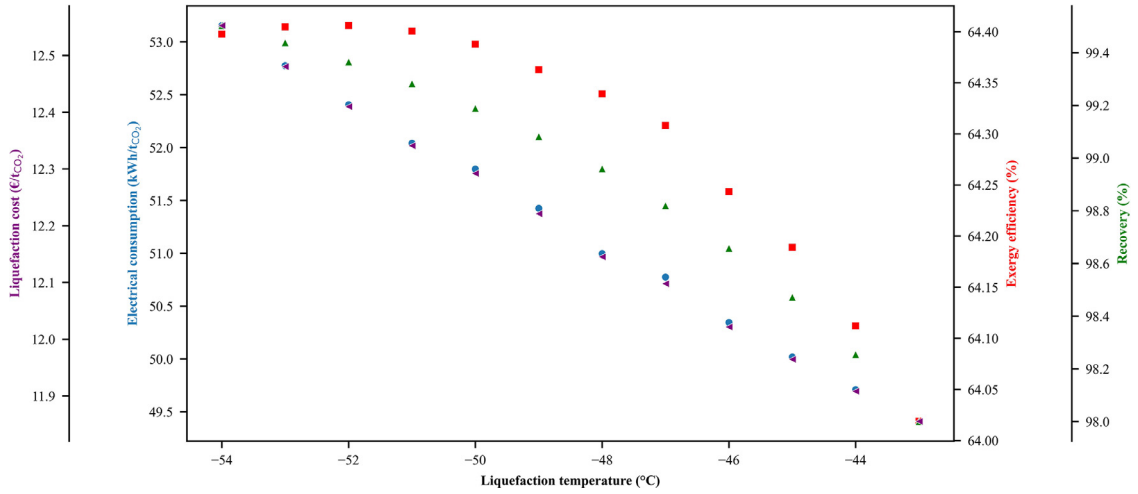

Fig. 11. KPIs in function of the liquefaction temperature for the closed cycle considering complete liquefaction at intermediate stage.

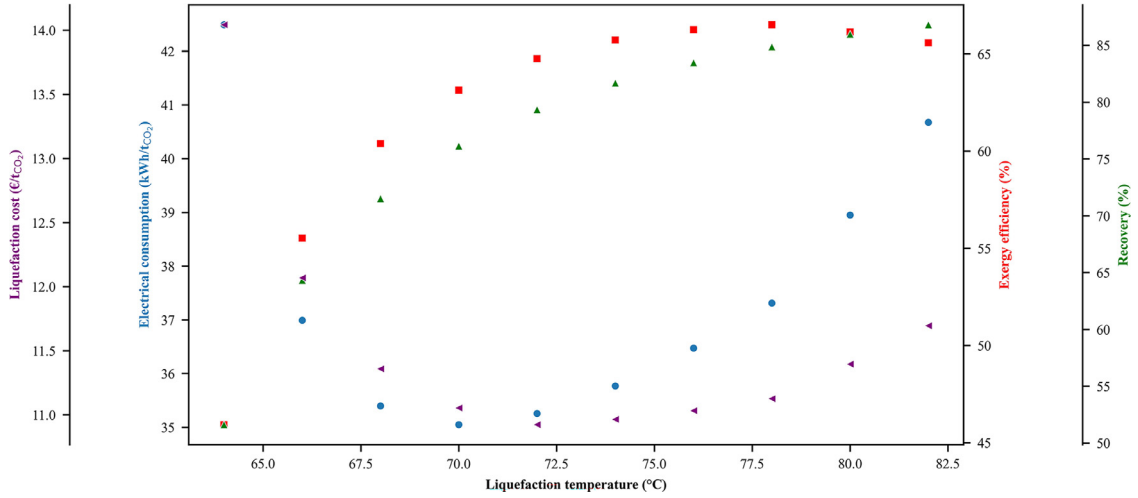

Fig. 12. KPIs in function of the liquefaction pressure for the open cycle.

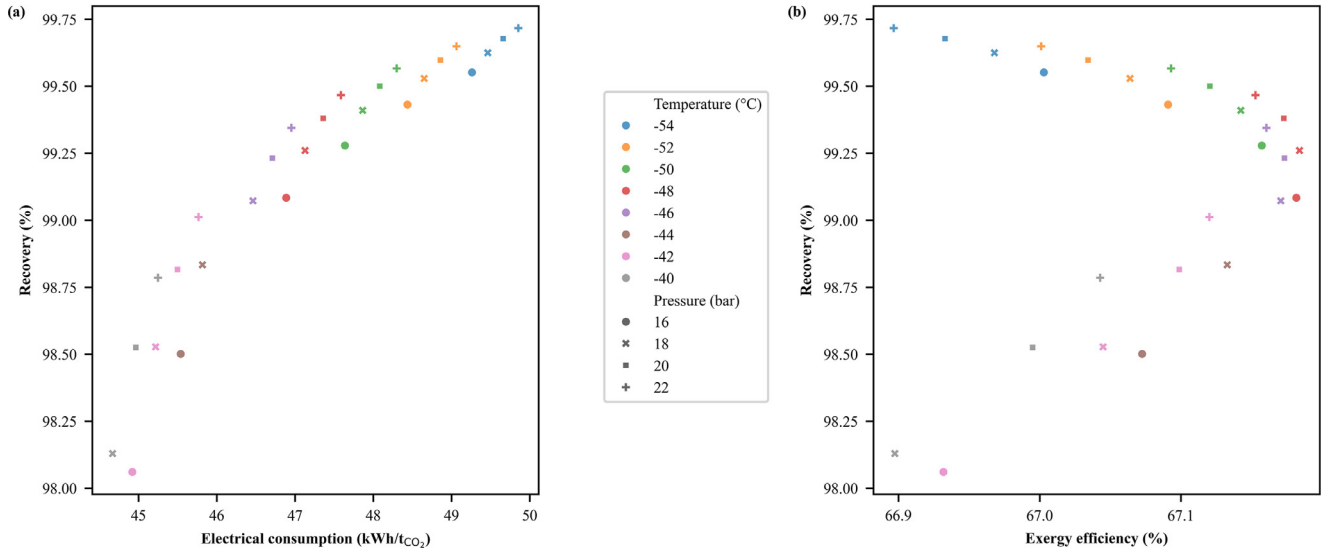

Fig. 13. KPIs (electrical consumption (a) and exergy efficiency (b) in function of the liquefaction temperature and pressure for the hybrid cycle considering complete liquefaction at intermediate stage.

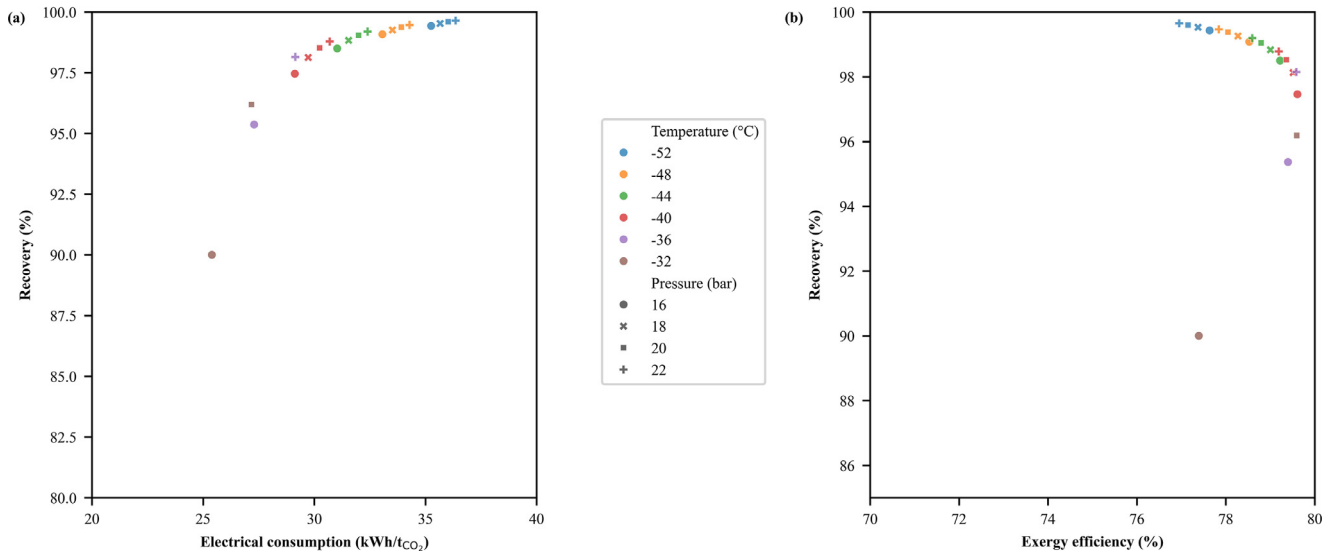

Fig. 14. KPIs in function of the liquefaction temperature and pressure for the hybrid cycle.

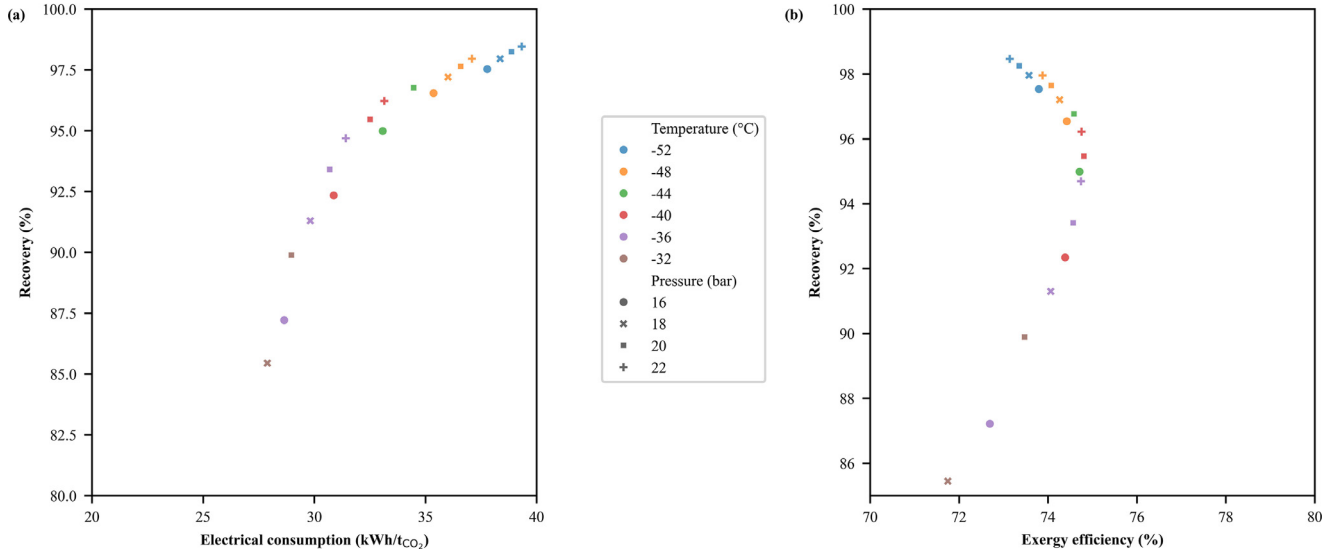

Fig. 15. KPIs in function of the liquefaction temperature and pressure for the hybrid cycle for Case 2.

The investigation of Case 2 shows an increase in electrical consumption as well as a significant loss of CO_2 through purges. However, there is also another significant criterion, which is the validation of the purity of the liquefied CO_2 compared to the specifications for the ship transportation. Among the different compounds that have specifications higher than those accepted in maritime transport by ship, only oxygen and carbon monoxide fall below the limit value for 6 of the 42 points simulated. Other components, on the other hand, consistently exceed the set limits. To meet the standards imposed for ship transportation, a further purification step (classically by distillation) of the liquid CO_2 is necessary to extract the dissolved gases and make it compliant with these specifications.

3.3.3. *Liquid CO_2 distillation as purification step for the case 2*

To meet the specifications required for transportation by ship, it is necessary to apply a distillation step to the liquid CO_2 to achieve the specified minimum purity. Given the previously obtained results showing that the hybrid cycle adapts well to impurities, a distillation column is added to it (as shown in the Fig. 6). Table 7 includes the various process variables for optimization. Distillation column is discretized into 20 stages that are used to determine the feed stage. The addition of additional variables implies a multimodal response that prevents the effective use of the Aspen Plus® optimizer tool. A genetic algorithm (NGSA-II) is employed using the Pymoo library (Blank and Deb, 2020) in Python.

Table 7
Optimization variables for hybrid cycle with distillation column.

Variable	Unit	Lower bound	Upper bound
Packing height	m	1	15
Column feed stage	–	5	15
Boil up ratio	mol/h/mol/h	0	1
Column pressure	bar	15	25
Condenser temperature	°C	−54	−28
HX2 vapor fraction	–	0	0.25

The Fig. 16 illustrates the various consumptions as a function of recovery for the different cases studied in this work. It can be observed that distillation of CO_2 achieving the specified targets for transportation by ship for case 2 consumes up to 16 % more electricity than for

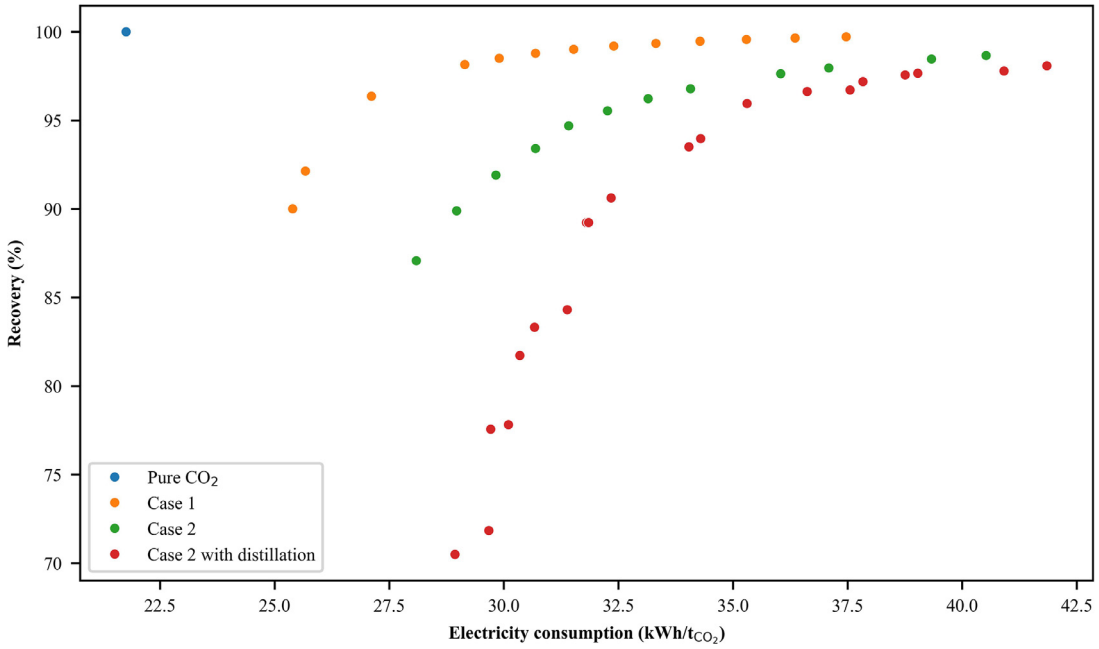

Fig. 16. Recovery in function of electrical consumption of hybrid cycle for the different cases.

the initial process with flash, which results in out-of-spec liquid CO_2. Looking at the figures obtained for the same conditions (inlet pressure, cooling water temperature, outlet pressure), it can be noticed that the consumption is almost double when seeking to minimize CO_2 losses.

Considering the case with different impurities in the CO_2 during transportation by pipeline, there is a loss of at least 2 % of the CO_2 regardless of the energy consumption. This limit is related to the minimum achievable temperature for CO_2. The condenser temperature tends to decrease from −30 °C to −54 °C as the recovery rate increases, implying higher electrical consumption to reach these colder temperatures at the refrigeration unit. Conversely, the column pressure is quite low for lower recoveries and increases for higher recoveries, ranging from 16 bar to 25 bar. For other column parameters, their variations tend to increase or decrease depending on the recovery rate, with the boil up rate ranging from 0.11 to 0.18, the packing height ranging from 1 to 8 m, and the feed stage varying between 5 and 7 considering a discretization of 20 stages. Finally, the vapor fraction at the outlet of the first liquefaction stage decreases from 0.24 to 0.17 for high recoveries (> 95 %).

3.4. Influence of the CO_2 losses on the total cost

Considering the carbon tax for CO_2 loss through the purge stream, an optimum can be determined for a CO_2 recovery value. Per ton of CO_2, the total cost, including the CO_2 capture costs and the carbon tax, can therefore be calculated as follows:

$$Total\ cost = \frac{CO_2\ recovery}{100} CO_2\ capture\ cost + \frac{(100 - CO_2\ recovery)}{100} carbon\ tax \quad (18)$$

In 2023, carbon tax of EU-ETS fluctuated between 77.39 and 100.34 €/t_{CO2} (Anon., EMBER 2023). The interval of the carbon tax is considered between 60 and 100 €/t_{CO2} in this study. The evolution of total cost for the more stringent gas operator specification case as a function of recovery and carbon tax for various concentrations is presented in Fig. 17. For the case at 60 €/t_{CO2}, the economic optimum is around 2.5 % loss of CO_2 during liquefaction. For case 1, the trend to minimize losses is the same, with however an optimum at 0.8 % loss for 100 €/t_{CO2}. This analysis demonstrates that it is interesting, knowing that the carbon tax will inevitably increase to achieve zero carbon emissions objectives, to minimize losses by increasing performance and therefore the cost of the process.

When comparing the costs associated with case 2, both with and without a distillation column, there is an observed increase in pricing ranging from approximately 7 % to 10 %. This upward cost trend can be attributed to the heightened electrical consumption and an additional investment, namely the inclusion of the distillation column. The price range for case 2, incorporating distillation, fluctuates between 12 and 13 €/t_{CO2}. In contrast, the cost for a pure CO_2 stream under identical conditions stands at 7.3 €/t_{CO2}.

The increase is noteworthy. This prompts a critical examination of the pipeline specifications, raising the question of whether they should align more closely with those typically associated with shipping methods.

3.5. Environmental impact of the electricity source

The electricity source used in the liquefaction process is a crucial factor in the context of reducing the overall carbon footprint of the CCUS chain. The choice of electricity source directly influences the global emissions associated with the liquefaction process. When electricity is generated from fossil fuels, the associated emissions can significantly reduce the overall effectiveness of CO_2 capture and storage efforts as show in studies (Costa et al., 2024b). Incorporating renewable energy, such as wind, solar, or hydropower, not only reduces greenhouse gas emissions but also enhances the long-term viability of CCUS technologies by mitigating reliance on non-renewable energy sources. Moreover, the transition to greener electricity can support the achievement of net-zero emission targets by ensuring that the process of capturing and storing CO_2 does not inadvertently contribute to the problem it aims to solve.

Different energy sources produce varying amounts of CO_2 depending on their nature. CO_2 avoided (Eq. (19)) refers to the CO_2 liquefied, minus the CO_2 emitted during electricity generation.

$$CO_2\ avoided = \frac{CO_2\ liquefied - CO_2\ emitted\ by\ power\ production}{CO_2\ flue\ gas} \quad (19)$$

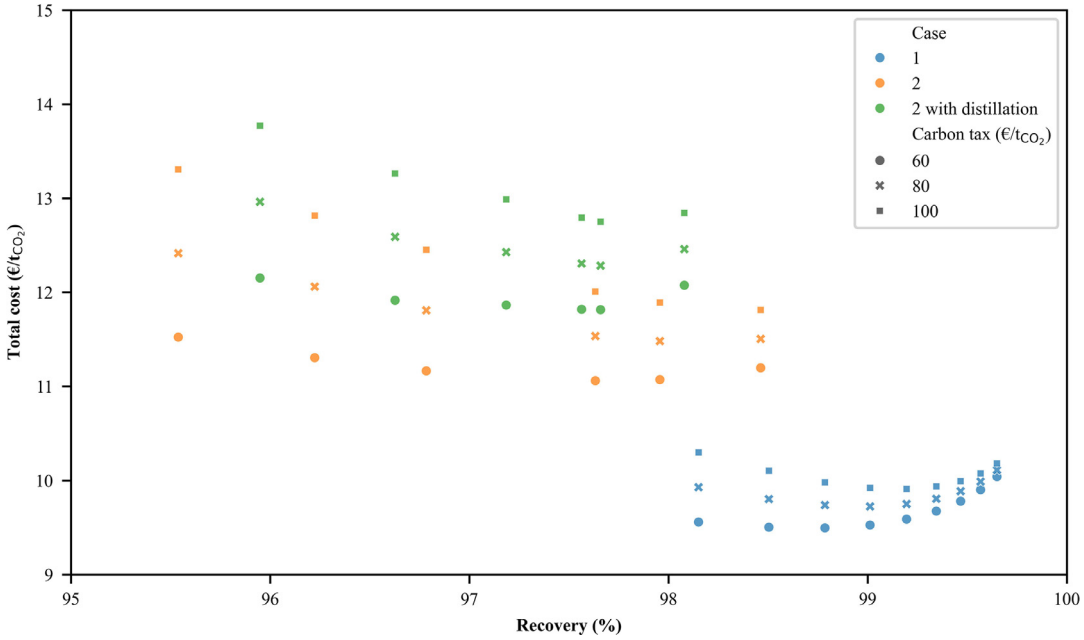

Fig. 17. Evolution of total cost as a function of CO_2 recovery and carbon tax for both case.

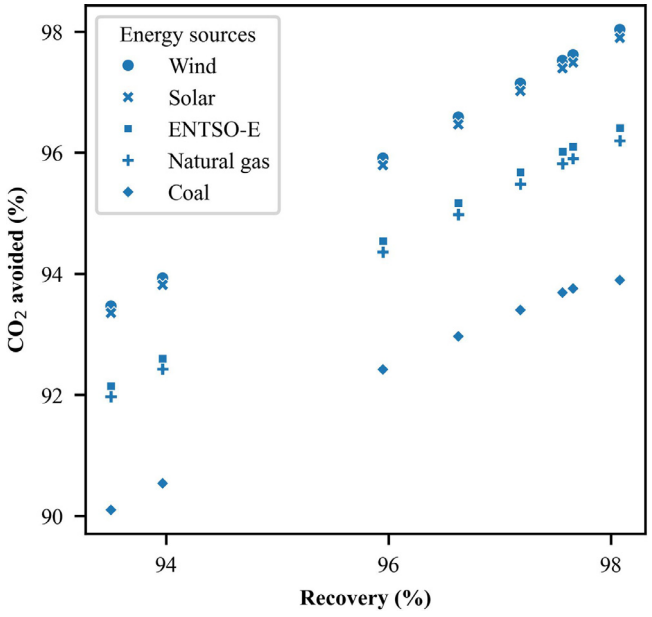

Fig. 18. CO_2 avoided as a function of CO_2 recovery for the case 2 with distillation. (Emissions factor (from (Coppitters et al., 2023)) of electricity (kg_{CO2e}/kWh): Wind = 0.011; European Network of Transmission System Operators (ENTSO-E) = 0.399; Natural gas = 0.450; Coal = 1.000).

The Fig. 18 illustrates the CO_2 avoided in function of the CO_2 recovery for different energy sources. It can be noted that at 98 % recovery, for ENTSO-E and natural gas, 2 % of CO_2 are lost, while for coal, a little more than 4 % of CO_2 are lost. A more significant change in the slope can be observed beyond 97.5 % recovery. These observations show that the source of electricity has a considerable impact on the carbon balance of the CCUS chain. However, in the case of a scenario involving transport by ship, it is important not to overlook the emissions related to fuel consumption, which are negligible in the context of transport by pipeline. The global CO_2 emissions of the full CCUS chain must be considered to assess the real impact of the CCUS solution.

4. Conclusion

Based on the comprehensive analysis conducted on the carbon capture, transport and storage, several key insights emerge regarding the optimal strategies and configurations for minimizing energy consumption and avoiding CO_2 losses.

The sensitivity study on cooling water temperature rise revealed a delicate balance between temperature increase and flow rate, with an optimal 7 °C rise for the closed cycle and 5 °C for the open cycle. This optimization minimizes liquefaction costs while considering electrical consumption and operational expenses.

In the simulation of pure CO_2 processes, it was observed that different cycles exhibit comparable electrical consumption, with variations influenced by cooling water temperatures and inlet pressures. Notably, the open cycle demonstrated superiority at lower cooling water temperatures, while refrigerants like ammonia proved advantageous, particularly as temperatures increased.

When considering CO_2 with impurities, adjustments in liquefaction parameters are essential to prevent dry ice formation and optimize CO_2 recovery. The closed cycle exhibited decreased energy consumption with higher liquefaction temperatures, whereas the open cycle's performance was affected by compressor pressure variations. The hybrid cycle emerged as a promising solution, offering lower energy consumption and improved CO_2 recovery compared to both closed and open cycles. By introducing additional degrees of freedom, such as adjustments in both temperature and pressure, the hybrid cycle enables precise control over variables, leading to enhanced efficiency and reduced CO_2 losses.

Overall, the hybrid cycle standing out as a versatile and efficient solution for addressing the complexities of CO_2 purification and liquefaction from pipeline. These insights contribute to advancing the development of sustainable practices in carbon capture, furthering efforts towards mitigating climate change.

To meet the specifications for transportation by ship, it is necessary to add a distillation column to the liquefaction process. The impurities and the column entail an additional consumption compared to a pure CO_2 case, almost doubling from 21.8 kWh/t_{CO2} to 40.9 kWh/t_{CO2} for a recovery of 98.1 %. Regarding the cost of the liquefaction, it is between 7 and 14 $€/t_{CO2}$ depending on the impurities present in the CO_2. In comparison to the other part of the CCS chain, this cost represents between

2 and 10 %. This range in cost highlights the significant impact that impurities can have on the overall expense of CO_2 liquefaction. The impurities also result in a loss of CO_2, which will be chargeable to the CO_2 liquefaction operator. A perspective of this work will be to study the chain in a more comprehensive manner to ultimately determine which is more economically viable: being stricter on the purity of CO_2 in the pipeline and thus increasing CO_2 purification at the capture unit exit, or sticking to current specifications, which involves treating the CO_2 from the pipeline to meet the specifications for ship transportation.

Declaration of competing interests

The authors declare the following financial interests/personal relationships which may be considered as potential competing interests:

Costa Alexis reports financial support was provided by University of Mons Faculty of Engineering. Lionel Dubois reports financial support was provided by University of Mons Faculty of Engineering. If there are other authors, they declare that they have no known competing financial interests or personal relationships that could have appeared to influence the work reported in this paper.

CRediT authorship contribution statement

Alexis Costa: Writing – review & editing, Writing – original draft, Visualization, Software, Methodology, Investigation, Data curation, Conceptualization. **Lionel Dubois:** Writing – review & editing. **Diane Thomas:** Writing – review & editing. **Guy De Weireld:** Writing – review & editing, Supervision.

Acknowledgements

The authors acknowledge the SPF Economie (Belgium) for funding the DRIVER project in the framework of the Energy Transition Fund program.

References

Alabdulkarem, A., Hwang, Y., Radermacher, R., 2012. Development of CO_2 liquefaction cycles for CO_2 sequestration. Appl. Therm. Eng. 33–34, 144–156. doi:10.1016/j.applthermaleng.2011.09.027.

Belgium, F. Information Memorandum for CO2 infrastructure, 2022. www.climat.be.

Blank, J., Deb, K., 2020. Pymoo: multi-Objective Optimization in Python. IEEe Access. 8, 89497–89509. doi:10.1109/ACCESS.2020.2990567.

Chauvy, R., Dubois, L., Lybaert, P., Thomas, D., De Weireld, G., 2020. Production of synthetic natural gas from industrial carbon dioxide. Appl. Energy 260, 114249. doi:10.1016/J.APENERGY.2019.114249.

Chen, F., Morosuk, T., 2021. Exergetic and economic evaluation of CO_2 liquefaction processes. Energies. (Basel) 14, 7174. doi:10.3390/en14217174.

Coppitters, D., Costa, A., Chauvy, R., Dubois, L., De Paepe, W., Thomas, D., De Weireld, G., Contino, F., 2023. Energy, exergy, economic and environmental (4E) analysis of integrated direct air capture and CO2 methanation under uncertainty. Fuel 344, 127969. doi:10.1016/J.FUEL.2023.127969.

Costa, A., Coppitters, D., Dubois, L., Contino, F., Thomas, D., De Weireld, G., 2024a. Energy, exergy, economic and environmental (4E) analysis of a cryogenic carbon purification unit with membrane for oxyfuel cement plant flue gas. Appl. Energy 357, 122431. doi:10.1016/j.apenergy.2023.122431.

Costa, A., Henrotin, A., Heymans, N., Dubois, L., Thomas, D., De Weireld, G., 2024b. Multi-objective optimization of a hybrid carbon capture plant combining a Vacuum Pressure Swing Adsorption (VPSA) process with a Carbon Purification unit (CPU). Chem. Eng. J. 493, 152345. doi:10.1016/J.CEJ.2024.152345.

Daud, N.K., 2021. Effects of CO_2 binary mixtures on pipeline performance for Carbon Capture and Storage. In: Mater Today Proc. Elsevier Ltd, pp. 861–865. doi:10.1016/j.matpr.2021.02.433.

de Kler, R., Neele, F., Nienoord, M., Brownsort, P., Koornneef, J., Belfroid, S., Peters, L., van Wijhe, A., Loeve, D. Transportation and unloading of CO2 by ship - a comparative assessment, 2015. https://www.researchgate.net/publication/303034150.

de Visser, E., Hendriks, C., Barrio, M., Mølnvik, M.J., de Koeijer, G., Liljemark, S., Le Gallo, Y., 2008. Dynamis CO_2 quality recommendations. Int. J. Greenhouse Gas Control 2, 478–484. doi:10.1016/j.ijggc.2008.04.006.

Deng, H., Roussanaly, S., Skaugen, G., 2019. Techno-economic analyses of CO_2 liquefaction: impact of product pressure and impurities. Int. J. Refrigeration 103, 301–315. doi:10.1016/J.IJREFRIG.2019.04.011.

Durusut, E., Joss, M. Shipping CO2 - UK Cost Estimation Study, 2018.

EMBER, Carbon Price Tracker, (2023). https://ember-climate.org/data/data-tools/carbon-price-viewer/ (accessed March 13, 2023).

Engel, F., Kather, A., 2017. Conditioning of a pipeline CO_2 stream for ship transport from various CO_2 sources. In: Energy Procedia. Elsevier Ltd, pp. 6741–6751. doi:10.1016/j.egypro.2017.03.1806.

Engel, F., Kather, A., 2018. Improvements on the liquefaction of a pipeline CO_2 stream for ship transport. Int. J. Greenhouse Gas Control 72, 214–221. doi:10.1016/J.IJGGC.2018.03.010.

Equinor, Northern Lights Project Concept report, 2019. www.equinor.com.

Fluxys, Carbon Specification Proposal Fluxys Belgium SA, 2022.

Gao, K., Wu, J., Bell, I.H., Harvey, A.H., Lemmon, E.W., 2023. A reference equation of state with an associating term for the thermodynamic properties of ammonia. J. Phys. Chem. Ref. Data 52. doi:10.1063/5.0128269.

Gong, W., Remiezowicz, E., Fosbøl, P.L., von Solms, N., 2022. Design and Analysis of Novel CO_2 Conditioning Process in Ship-Based CCS. Energies. (Basel) 15. doi:10.3390/en15165928.

Huber, M.L., Lemmon, E.W., Bell, I.H., Mclinden, M.O., 2022. The NIST REFPROP Database for Highly Accurate Properties of Industrially Important Fluids. Ind. Eng. Chem. Res. 61, 15449–15472. doi:10.1021/acs.iecr.2c01427.

IEA, Transforming Industry through CCUS, 2019.

IPCC, 2023. SYNTHESIS REPORT OF THE IPCC SIXTH ASSESSMENT REPORT (AR6). Panmao Zhai.

Jackson, S., Brodal, E., 2019. Optimization of the CO_2 liquefaction process-performance study with varying ambient temperature. Appl. Sci. (Switzerland) 9, 4467. doi:10.3390/app9204467.

Kegl, T., Čuček, L., Kovač Kralj, A., Kravanja, Z., 2021. Conceptual MINLP approach to the development of a CO_2 supply chain network – Simultaneous consideration of capture and utilization process flowsheets. J. Clean. Prod. 314. doi:10.1016/j.jclepro.2021.128008.

Lee, U., Yang, S., Jeong, Y.S., Lim, Y., Lee, C.S., Han, C., 2012. Carbon dioxide liquefaction process for ship transportation. Ind. Eng. Chem. Res. 51, 15122–15131. doi:10.1021/ie300431z.

Lemmon, E.W., McLinden, M.O., Wagner, W., 2009. Thermodynamic properties of propane. III. A reference equation of state for temperatures from the melting line to 650 K and pressures up to 1000 MPa. J. Chem. Eng. Data 54, 3141–3180. doi:10.1021/je900217v.

Li, H., Yan, J., Yan, J., Anheden, M., 2009. Impurity impacts on the purification process in oxy-fuel combustion based CO_2 capture and storage system. Appl. Energy 86, 202–213. doi:10.1016/j.apenergy.2008.05.006.

Martynov, S.B., Daud, N.K., Mahgerefteh, H., Brown, S., Porter, R.T.J., 2016. Impact of stream impurities on compressor power requirements for CO2 pipeline transportation. Int. J. Greenhouse Gas Control 54, 652–661. doi:10.1016/j.ijggc.2016.08.010.

Mathias, P.M., Copeman, T.W., 1983. Extension of the Peng-Robinson equation of state to complex mixtures: evaluation of the various forms of the local composition concept. Fluid. Phase Equilib. 13, 91–108. doi:10.1016/0378-3812(83)80084-3.

Maxwell, C. Cost Indices, (2022). https://www.toweringskills.com/financial-analysis/cost-indices/ (accessed August 30, 2022).

Mazzoccoli, M., Bosio, B., Arato, E., 2012. Analysis and comparison of equations-of-state with p-ρ-T experimental data for CO2 and CO2-Mixture Pipeline Transport. Energy Procedia 23, 274–283. doi:10.1016/J.EGYPRO.2012.06.052.

Moe, A.M., Dugstad, A., Benrath, D., Jukes, E., Anderson, E., Catalanotti, E., Durusut, E., Neele, F., Grunert, F., Mahgerefteh, H., Gazendam, J., Barnett, J., Hammer, M., Span, R., Brown, S., Tollak Munkejord, S., Weber, V. A trans-European CO2 transportation infrastructure for CCUS: opportunities & challenges, 2020.

Nilsson, P.A., Apeland, S., Dale, H.M., Decarre, S., Eldrup, N.H., Hansen, H.-R., Nilsson, J.-A., Rennie, A., Skagestad, R., Wendt, T. The costs of CO2 transport: post-demonstration CCS in the EU, 2011.

Northern Lights, Liquid CO2 Quality Specifications, 2024.

Oei, P.-Y., Mendelevitch, R. Development scenarios for a CO2 infrastructure network in Europe, 2013. https://www.researchgate.net/publication/259998544.

Phillips, I., Tucker, A., Granstrom, P.-O., Bozzini, G., Gent, C., Capello, P.J., Clifton, A., Clucas, C., Dolek, B., Duclos, P.-Y., Faou, M., Fletcher, D., Todd, J., Metcalf, C., Neele, F., Reid, M., Senkel, J., Simpson, J., StigterTrevor Crowe, H., Versteele, W., Wong, S. Network technology: guidance for CO2 transport by ship, 2022.

Psarras, P., He, J., Pilorgé, H., Mcqueen, N., Jensen-Fellows, A., Kian, K., Wilcox, J. Part 1: cost analysis of carbon capture and storage from U.S. Natural gas-fired power plants, 2020.

Remy, L., Cornelis, J., Schalck, D. Fluxys, ArcelorMittal Belgium and North Sea Port move forward to foster decarbonisation in Belgium, (2022). https://www.fluxys.com/en/press-releases/fluxys-group/2022/220818_press_ghent_carbon_hub (accessed September 8, 2022).

Rivero, R., Garfias, M., 2006. Standard chemical exergy of elements updated. Energy 31, 3310–3326. doi:10.1016/J.ENERGY.2006.03.020.

Roussanaly, S., Deng, H., Skaugen, G., Gundersen, T., 2021. At what pressure shall CO_2 be transported by ship? An in-depth cost comparison of 7 and 15 barg shipping. Energies. (Basel) 14. doi:10.3390/en14185635.

Seo, Y., You, H., Lee, S., Huh, C., Chang, D., 2015. Evaluation of CO2 liquefaction processes for ship-based carbon capture and storage (CCS) in terms of life cycle cost (LCC) considering availability. Int. J. Greenhouse Gas Control 35, 1–12. doi:10.1016/j.ijggc.2015.01.006.

Seo, Y., Huh, C., Lee, S., Chang, D., 2016. Comparison of CO_2 liquefaction pressures for ship-based carbon capture and storage (CCS) chain. Int. J. Greenhouse Gas Control 52, 1–12. doi:10.1016/j.ijggc.2016.06.011.

Svensson, R., Odenberger, M., Johnsson, F., Strömberg, L., 2004. Transportation systems for CO_2 - Application to carbon capture and storage. Energy Convers. Manage 45, 2343–2353. doi:10.1016/j.enconman.2003.11.022.

Szargut, J., 1989. Chemical Exergies of the Elements. Appl. Energy 32, 269–286. doi:10.1016/0306-2619(89)90016-0.

Turton, R., Shaeiwitz, J.A., Bhattacharyya, D., Whiting, W.B., 2018. Analysis, Synthesis, and Design of Chemical Processes. Pearson Education, Inc.

Wang, C., Seibert, A.F., Rochelle, G.T., 2015. Packing characterization: absorber economic analysis. Int. J. Greenhouse Gas Control 42, 124–131. doi:10.1016/j.ijggc.2015.07.027.

Wang, H., Chen, J., Li, Q., 2019. A review of pipeline transportation technology of carbon dioxide. IOP Conf Ser Earth Environ Sci. Institute of Physics Publishing doi:10.1088/1755-1315/310/3/032033.

Wetenhall, B., Race, J.M., Downie, M.J., 2014. The effect of CO_2 purity on the development of pipeline networks for carbon capture and storage schemes. Int. J. Greenhouse Gas Control 30, 197–211. doi:10.1016/j.ijggc.2014.09.016.

Zhang, Z.X., Wang, G.X., Massarotto, P., Rudolph, V., 2006. Optimization of pipeline transport for CO_2 sequestration. Energy Convers. Manage 47, 702–715. doi:10.1016/J.ENCONMAN.2005.06.001.

Zhang, S., Liu, L., Zhang, L., Zhuang, Y., Du, J., 2018. An optimization model for carbon capture utilization and storage supply chain: a case study in Northeastern China. Appl. Energy 231, 194–206. doi:10.1016/j.apenergy.2018.09.129.